Orally bioavailable Bruton's tyrosine kinase proteolysis-targeting chimeras active against wild-type and C481 mutant BTKs in murine hematology models

Ye Seul Lim
Ubix Therapeutics
Sun-Mi Yoo
Ubix Therapeutics
Vineet Patil
Korea Research Institute of Chemical Technology
Han Wool Kim
Ubix Therapeutics
Hyun-Hwi Kim
Ubix Therapeutics
Beomseon Suh
Ubix Therapeutics
Ji Youn Park
Ubix Therapeutics
Na-rae Jeong
Ubix Therapeutics
Chi Hoon Park
Korea Research Institute of Chemical Technology
Je Ho Ryu
Ubix Therapeutics
Byung-Hoon Lee
Daegu Gyeongbuk Institute of Science and Technology (DGIST)
Pilho Kim
Korea Research Institute of Chemical Technology
Song Hee Lee (shlee@ubixtrx.com)
Ubix Therapeutics

Research Article

Keywords: Bruton's tyrosine kinase, B-cell receptor, B-cell malignancy, proteolysis, PROTAC

Posted Date: April 11th, 2022

DOI: https://doi.org/10.21203/rs.3.rs-1528349/v1

Abstract

Background

Bruton's tyrosine kinase (BTK) is an important signaling hub that activates the B-cell receptor (BCR) signaling cascade. BCR activation can contribute to the growth and survival of B-cell lymphoma or leukemia. The inhibition of the BCR signaling pathway is critical for blocking downstream events and treating B-cell lymphomas. Herein, we report potent and orally available proteolysis-targeting chimeras (PROTACs) that target BTK to inactivate BCR signaling.

Methods

Fluorescence resonance energy transfer signals were used to assess BTK and cereblon (CRBN) ternary complex formation with Mab anti-6His-Eu cryptate and Mab anti-glutathione-S-transferase-XL665. BTK and CRBN binding activities were investigated using *in vitro* target binding assays. Subsequently, SDS-PAGE and western blotting of whole cell lysates was performed, followed by immunofluorescence analysis of TMD-8 cells. ELISA was performed in TMD-8 cells treated with 0.01 μM PROTAC, ibrutinib, acalabrutinib, ARQ-531, Binder, or MT-802 to measure CCL3 and CCL4 levels. Tandem ubiquitin-binding elements pull-down assay was used to characterize UBX-382 in Ramos cells. Various cells treated with inhibitor or PROTAC were assessed for proliferation and viability. Wild-type- or BTK-transfected cells were transplanted in CB17/SCID mice and the established tumors were assessed using immunohistochemistry.

Results

Of the PROTACs tested, UBX-382 showed superior degradation activity for wild-type (WT) and mutant BTK proteins in a single-digit nanomolar range of DC_{50} in DLBCL cell line. UBX-382 was effective on seven out of eight known BTK mutants in *in vitro* experiment and was highly effective in inhibiting tumor growth in murine xenograft models harboring WT or C481S mutant BTK-expressing TMD-8 cells over ibrutinib, ARQ-531, and MT-802. Remarkably, oral dosing of UBX-382 for less than 2-weeks led to complete tumor regression in 3 and 10 mg/kg groups in murine xenograft models. UBX-382 also provoked the cell-type-dependent and selective degradation of CRBN neo-substrates in various hematological cancer cells.

Conclusions

These results suggest that UBX-382 treatment is a promising therapeutic strategy for B-cell-related blood cancers with improved efficacy and diverse applicability.

Background

Non-Hodgkin's lymphoma is a major type of B-cell-associated hematological cancer with which 81,560 individuals were diagnosed during 2021 in the US according to the American Cancer Society [1]. Bruton's tyrosine kinase (BTK) is a non-receptor tyrosine kinase belonging to the Tec family and plays a critical role in B-cell development and adaptive immune response [1, 2]. B-cell receptor (BCR) activation is the first step in the signaling cascade that triggers activation of kinases, such as BTK, SYK, and PI3Kδ, in the plasma membrane [3]. BTK promotes the nuclear localization of NF-κB, which leads to transcriptional activation of target genes that can trigger the development, survival, and proliferation of B cells [4]. Aberrant or dysregulated BTK activity has been intimately associated with B-cell malignancies [5]. Hence, the inhibition of BTK has been emerged as one of the major strategies that can treat B cell-related hematological cancers.

Ibrutinib, a first-in-class BTK inhibitor, has been approved by the Food and Drug Administration (FDA) and European Medicines Agency for the treatment of B-cell malignancies including chronic lymphocytic leukemia/small lymphocytic lymphoma (CLL/SLL), Waldenström's macroglobulinemia (WM), relapsed/refractory mantle cell lymphoma (R/R MCL), and relapsed/refractory marginal zone lymphoma (R/R MZL) [6, 7]. Acalabrutinib and zanubrutinib, second-generation BTK inhibitors, appear to have fewer off-target or adverse effects than ibrutinib [8, 9]. However, resistance to these irreversible inhibitors has been reported mainly in CLL and MCL patients [10, 11]. Genomic sequencing analysis of CLL patients who exhibited relapse under treatment with ibrutinib revealed mutations in the *BTK* gene [12]. Notably, the most frequent mutation was the substitution of the cysteine 481 residue with serine [13]. The C481 residue plays a critical role in the covalent binding of irreversible BTK inhibitors approved and the BTK protein, thus this mutation prevents the irreversible and covalent binding of these drugs, resulting in drug resistance [12, 14]. Thus, novel therapeutic options are required to overcome the drug resistance issue.

Proteolysis-targeting chimeras (PROTACs), heterobifunctional molecules that induce target protein degradation through the ubiquitin-proteasome system (UPS), have emerged as a new strategic technology in drug discovery [15, 16]. PROTACs are structurally composed of three elements: a warhead ligand that binds to the target protein, a ligand that binds to the E3 ubiquitin ligase, and a linker that couples the two ligands [17]. A PROTAC could generate proximity between E3 ligase and the protein of interest (POI), thus forming a ternary complex (POI:PROTAC:E3), which can efficiently induce ubiquitination and promote the degradation of the POI via the proteasome [16, 18]. Since its introduction in 2001 [16], PROTAC technology has innovated the concept of conventional druggability [19]. Thus far PROTACs could expand target space by degrading various proteins such as AR, ERα, BRD2•3•4, FKBP12, BCR-ABL, HCV NS3/4A. In addition, diverse E3 ligases such as von Hippel-Lindau (VHL), cereblon (CRBN), and inhibitors of apoptosis have been utilized for PROTACs [20–25]. CRBN E3 ligase binders were originally developed as immunomodulatory drugs (IMiDs) such as thalidomide, pomalidomide, lenalidomide, CC-122, and CC-885. These binders enable CRBN E3 ligase to degrade neo-substrates such as Ikaros (IKZF1), Helios (IKZF2), Aiolos (IKZF3), casein kinase 1-a (CK1-a), and G1 to S phase transition

protein 1 (GSPT1) [26]. CRBN binders have been widely used in designing various PROTACs owing to its ligand availability and well-characterized structure.

PROTACs offer several advantages compared to traditional inhibitors. Conventional small-molecule inhibitors operate via occupancy-driven pharmacology, meaning that their efficacy is determined by long-term binding to active sites, which inactivates the target functions [27]. On the other hand, protein degraders are characterized as event-driven mechanisms, meaning that they are competent for proteolytically targeting the protein substrate, even under a transient binding [28]. Since PROTACs can utilize both the allosteric binding sites and the active sites of target proteins, they possess great potential to degrade undruggable proteins, such as transcription factors, non-enzyme proteins, and scaffolding proteins [29]. Furthermore, PROTACs may overcome drug resistance by eliminating overexpressed or mutated target proteins, even those with low binding affinity [30]. Therefore, PROTAC-mediated protein degradation could be a promising strategy in drug development.

In this context, various BTK PROTACs, such as MT-802, P13I, BGB-16673 and HSK29116 have been reported to develop novel options for the treatment of hematological cancers [31]. NX-2127, which is recently being developed by Nurix therapeutics as an oral administration PROTAC showing BTK protein degradation effect, has entered phase 1 clinical trials for B cell-related blood cancers (CLL, SLL, WM, MCL, MZL, FL, and DLBCL patients). NX-2127 showed moderately effective tumor growth inhibition at the same dose of ibrutinib in the BTK wild-type (WT) xenograft murine model, and more potent tumor growth suppression compared to ibrutinib in the BTK C481S mutant model, but the tumor was not completely regressed in the murine models.

In this study, we report UBX-382 as a potent BTK PROTAC that exhibits extraordinary efficacy in targeting BTK and inhibiting BCR signaling in hematological malignancies. UBX-382 showed inhibitory effects on tumor growth resulting from both wild-type and mutated BTK overexpression in *in vitro* and *in vivo* models. Moreover, UBX-382 also revealed selective degradation patterns for CRBN-IMiD neo-substrates such as Ikaros/Aiolos and GSPT1 in diverse hematological cancers, which probably reflects their diverse responses to UBX-382 treatment considering tumor growth inhibition.

Methods

In vitro ternary complex formation assay

The assay was performed by combining histidine-tagged BTK (His-BTK, Thermo Fisher, PV3363), glutathione-S-transferase (GST)-tagged CRBN (Abnova, H00051185), Mab anti-6His-Eu cryptate (Cisbio, 61HISKLA), and Mab anti-GST-XL665 (Cisbio, 61GSTXLF) in a buffer (50 mM HEPES (N-2-hydroxyethylpiperazine-N'-2-ethanesulfonic acid) pH 7.5, 10 mM $MgCl_2$, 1 mM EGTA, 0.01% Brij-35). Fluorescence resonance energy transfer (FRET) signals were collected at 620 nm (Eu, donor) and 665 nm (XL665, acceptor), and dose–response curves were obtained by increasing PROTAC concentrations to donor–BTK and acceptor–conjugates in a final assay volume of 25 µL using a 384-well low-volume

plate. The relative FRET signal was at a ratio of 665:620 and normalized against the maximum signal for the PROTAC.

In vitro target binding assay

The binding assay for WT-BTK was performed using the Lantha Screen^{TM} Eu kinase binding assay kit (Thermo Fisher) per the manufacturer's protocol with some modifications. The assay was performed on white 384-well microplates (Corning, 6008280) in a buffer (50 mM HEPES pH 7.5, 10 mM $MgCl_2$, 1 mM EGTA, 0.01% Brij-35) by mixing the final concentrations of 5 nM BTK (Thermo Fisher, PV3363), 30 nM Kinase Tracer 236 (Thermo Fisher, PV5592), and 2 nM Eu-anti-His-tag antibody (Thermo Fisher, PV5596) with compounds used. All compounds were prepared in duplicate to calculate half-maximal inhibitory concentration (IC_{50}) values. The mixture was incubated at room temperature (RT) and time-resolved FRET (TR-FRET) signals were collected at 615 nm (donor) and 665 nm (acceptor) using the Bio-Tek Synergy H1 microplate reader. IC_{50} values of the compounds were calculated against those of BTK using GraphPad Prism 5.

The homogeneous TR-FRET (HTRF) assay was performed to measure CRBN binding activity using a CRBN binding assay kit (Cisbio, 64BDCRBNPEG). The assay was performed by combining GST-tagged CRBN protein, Eu-anti-GST antibody, thalidomide-red, and serially diluted compounds in a Cisbio's PROTAC binding buffer using white 384-well microplates (Corning, 6008280). Following incubation at RT, the plate was read using a Bio-Tek Synergy H1 microplate reader. The HTRF signals were collected at 620 nm and 665 nm and calculated using the following equation: signal 665 nm/signal 620 nm × 10,000. GraphPad Prism 5 was used to plot dose–response curves and calculate IC_{50} values for each compound.

Sodium dodecyl sulfate–polyacrylamide gel electrophoresis (SDS-PAGE) and western blotting

Total lysates from TMD-8 were separated on SDS-PAGE gel. Proteins were transferred using Trans-Blot Turbo Transfer Kit. For conventional western blotting, membranes were blocked with 5% skim milk powder in Tris (tris(hydroxymethyl)aminomethane)-buffered saline and Tween 20 (TBST) (25 mM Tris pH 7.5, 150 mM NaCl, 0.2% Tween-20) for 45 min at RT, incubated overnight at 4°C with a primary antibody (anti-BTK, Cell Signaling Technologies, cat. #8547, 1:1,000 dilution in a blocking buffer), and washed thrice with TBST before adding anti-rabbit immunoglobulin (Ig) G (Cell Signaling Technologies, cat. #7074, 1:5,000 dilution in a blocking buffer) for 45 min at RT. The mixture was then washed thrice in TBST and developed by electrochemiluminescence (Super Signal Chemiluminescent Substrate, Thermo Fisher Scientific).

Western blotting was performed using LI-COR Odyssey® Infrared Imaging System. The experiments were performed per the manufacturer's instructions. Briefly, proteins were separated as described above alongside Odyssey pre-stained molecular weight markers (Licor, fluorescence in a 700-nm channel).

Immunofluorescence

The TMD-8 cells were fixed using 4% paraformaldehyde, washed with phosphate-buffered saline (PBS), and permeabilized with 0.25% Triton X-100. The cells were then washed with PBS and blocked with 1% bovine serum albumin/PBS with Tween 20. Coverslips were incubated overnight at 4°C with 1:250 anti-BTK (Cell Signaling Technologies, cat. #8547) and 1:50 anti-CRBN (R&D Systems, cat. MAB9574-100). The following day, the coverslips were washed with PBS and incubated with 200 µL of 1:500 a secondary anti-rabbit (Goat anti-rabbit IgG (H + L) Highly Cross-Adsorbed Secondary Antibody, Alexa Fluor Plus 488, cat. A32731) or anti-mouse antibody (goat anti-mouse IgG (H + L) cross-adsorbed secondary antibody, Alexa Fluor 647 cat: A21235) for 45 min in the dark. A fluorophore-conjugated secondary antibody was added to check positive signals using Zeiss LSM900 (Carl Zeiss).

Tandem ubiquitin-binding elements (TUBE1) pull-down assay

Ramos cells were seeded in a 150-mm dish and immediately treated with 0.1 µM of UBX-382 or vehicle for 2 h at 37°C. The cells were then lysed using 50 mM Tris-HCl (pH 7.5), 150 mM NaCl, 1 mM EDTA, 1% NP-40, 10% glycerol, supplemented with Protease/Phosphatase Inhibitor (5872S, Cell Signaling Technology) and deubiquitinase inhibitors (10 mM N-ethylmaleimide, 80 µM PR-619) for 10 min. The lysates were then cleared by centrifugation. Equal amounts of supernatants were then incubated with 30 µL agarose TUBE1 beads (UM401, Lifescience) at 4°C for 2 h. The beads were then collected by centrifugation, washed twice by re-suspending, and re-suspended in a 5X SDS buffer. The beads were then boiled for 5 min and analyzed by SDS-PAGE. Western blotting was performed per the standard protocols.

C-C motif chemokine ligand (CCL) 3 & CCL4 enzyme-linked immunosorbent assay (ELISA)

TMD-8 cells were seeded at 2×10^6 cells/well on a 12-well plate (Corning, CLS3513) in a 1 mL of cell culture medium and were treated with 0.01 µM PROTAC, ibrutinib, acalabrutinib, ARQ-531, Binder, or MT-802 for 24 h followed by stimulation with 10 µg/mL anti-IgM (Southern Biotech, 2022-01) for 8 h before harvesting. Supernatant from the TMD-8 cells was then collected to measure CCL3 and CCL4 levels using a human CCL3/MIP-1α Quantikine ELISA kit (R&D Systems, DMA00) and a human CCL4/MIP-1β Quantikine ELISA kit (R&D Systems, DMB00) per the manufacturer's instructions. Absorbance was detected using a Synergy H1 microplate reader (Bio-Tek) and Gen5 (version 3.08).

Cell proliferation

Cells (TMD-8, OCI-LY3, U2932, TMD-8 BTK WT, TMD-8 BTK C481S, WSU-DLCL2, Su-DHL10, DOHH2, MINO, Waldenström macroglobulinemia (WSU-WM), K562, and acute myeloid leukemia (MOLM13)) were seeded into 96-well microplates at 500–2000 cells/well. Cells were treated with inhibitor or PROTAC stocks at the final concentration and incubated for 5 days, followed by a cell viability assay performed using the Cell Titer-Glo® 2.0 assay kit (Promega, G9242) following the manufacturer's protocols. The plate and its contents were equilibrated at RT for 30 min before reagent addition. Cell Titer-Glo® 2.0 was added at equal volumes to the cell culture media in each well. Plates were mixed for 2 min to induce cell

lysis and incubated for 10 min at RT to stabilize the luminescent signal. The luminescent signal was measured using a microplate reader (Bio-Tek, Synergy H1). Data were analyzed using GraphPad Prism 5.

Stable cell line generation

pLVX-BTK WT or pLVX-BTK C481S plasmids were co-transfected with a packaging plasmid and VSV-G envelope plasmid into 293T cells. Lentiviral supernatant was collected at 48 h and added to the TMD-8 cells with polybrene 72 h after transfection (8 μg/mL). Puromycin (3 μg/mL) selection was performed for 2 weeks to produce TMD-8 BTK WT and TMD8 BTK C481S cell lines.

Transient transfection

HEK293 cells were seeded on 6-well plates and transfected with pCMV3-N-Flag BTK WT, E41K, T474I, T474S, C481S, C481R, C481F, C481Y, C481T, and L528W plasmids using Lipofector-EZ Reagent (APTABIO, AB-LF-EX150) per the manufacturer's protocol with modifications. For each transfection, 1.5 μg of plasmid and 4 μL of transfection reagent were added to 100 μL of a serum- and antibiotic-free medium. The mixture was incubated at RT for 15 min before adding it into the wells. The cells were incubated for 5 h before medium replacement. After 24 h, the transfected cells were reseeded onto a 12-well plate. Then, the cells were treated with UBX-382, ARQ-531, and MT-802 for 24 h. pCMV3-N-Flag BTK WT (Sino Biological, HG10578-NF) was purchased, whereas other BTK mutant vectors were generated by pCMV3-N-Flag BTK WT site-directed mutagenesis by Cosmo Genetech.

In vivo xenograft model

CB17/SCID mice were obtained from CLEA Japan, Inc. and were transplanted with TMD-8 cells at 6 weeks of age. The TMD-8 cells were subcutaneously injected into the mice at a dose of 1×10^7 cells/mice with Matrigel (Corning, 356237). Tumors reached an average volume of 180–200 mm^3 15 days after inoculation, after which the mice were divided into four groups based on tumor size. Vehicle control or UBX-382 was then administered orally at doses of 3, 10, or 30 mg/kg once a day for 21 days. The mice were observed for 8 weeks following the final administration for tumor rebound. Tumors and body weight were measured thrice per week using calipers (Mitutoyo, CD-15APX), and tumor volume was calculated using the formula: length × $width^2$ × 0.5.

Immunohistochemistry

Spleen tissues and TMD-8 xenografted tumors were extracted from mice, fixed in 4% paraformaldehyde, and paraffinized. Paraffin blocks were sectioned, deparaffinized with xylene, rehydrated, and treated with citrate for 1 h for antigen retrieval. After washing with PBS, the tissue sections were blocked with serum at RT and the blocked sections were incubated with a primary antibody against BTK antibody for 1 h. After washing with PBS, the sections were treated with H_2O_2 to block any endogenous peroxidase activity. The Envision Single Reagent (rabbit horseradish peroxidase) detection system (Dako, K4003) was used as a secondary antibody, and treatment was performed for 1 h. After development with 3,3-

diaminobenzidine for 30 min, the sections were counterstained with hematoxylin (ab220365; Abcam) for 1 min and subjected to alcohol dehydration and clearing with xylene before mounting and sealing on slides.

Results

Characterization of BTK PROTAC

Of the new BTK RPOTACs prepared, UBX-382 was selected as the most promising compound. The molecule contains a novel BTK binder, a short linker, and a known thalidomide-based CRBN binder. UBX-382-Me, an N-methylated analog of UBX-382, was synthesized as a negative control (Fig. 1A). An *in vitro* TR-FRET assay was performed by varying the concentration of each PROTAC to investigate the formation of the [BTK:PROTAC:CRBN] ternary complex. The Eu-anti-His-BTK and XL665-anti-GST-CRBN pair generates a FRET signal in close proximity, enabling the quantitative determination of the ternary complex formation upon treatment with UBX-382 or UBX-382-Me (Fig. 1B). The ternary complex formed readily as the concentration of UBX-382 increased; however, a hook effect became evident from the inflection points on the FRET curve owing to the dominance of the UBX-382:BTK and UBX-382:CRBN binary complexes at approximately 160 nM. As expected, UBX-382-Me did not show any FRET signals at any concentration (Fig. 1B). To determine the binding affinity of UBX-382, TR-FRET-based binding assays were performed to measure the IC_{50} values of seven compounds (UBX-382, UBX-382-Me, MT-802, ARQ-531, ibrutinib, thalidomide, and pomalidomide) in binding to BTK or CRBN. UBX-382 and UBX-382-Me showed approximately 10-fold lower binding affinities for BTK than the two BTK inhibitors ARQ-531 [32] and ibrutinib; however, the obtained IC_{50} values were still ~2 to 3 times higher than that of MT-802, a reported BTK PROTAC [31] (Fig. 1C). UBX-382 presented a binding affinity for CRBN in a micromolar range of IC_{50} that was comparable to other known CRBN ligands (thalidomide and pomalidomide) and MT-802 (Fig. 1D). As expected, UBX-382-Me, ARQ-531, and ibrutinib did not bind to CRBN (Fig. 1D). These results indicate that UBX-382 forms a functional ternary complex with BTK and CRBN E3 ligase to induce ubiquitination of BTK protein.

UBX-382 induces potent BTK degradation in B-cell lymphoma cell lines

To investigate the degradation activity of UBX-382, a concentration escalation assay of PROTAC was performed in the ABC-DLBCL cell line TMD-8 over 24 h. The levels of BTK protein were measured by quantitative western blotting, which yielded ~4 nM DC_{50} of UBX-382 (Fig. 2A). As expected, UBX-382-Me did not degrade BTK at any concentration. Next, Time-dependent BTK degradation was examined by treating the TMD-8 cells with UBX-382 over 0.5, 1, 4, 16, 24, and 48 h. The levels of BTK protein decreased rapidly to reach < 10 % after 4 h of treatment with 100 nM UBX-382 (Fig. 2B). To visualize the localization of BTK protein degraded by UBX-382, immunofluorescence was performed using confocal microscopy. The results indicated that BTK was mainly localized in the cytoplasm, as previously reported [33], and that UBX-382 treatment significantly reduced the BTK protein levels (Fig. 2C). To confirm whether the effect of UBX-382 is UPS-dependent, A TUBE1 pull-down assay was performed to

capture the ubiquitinated conjugates [34]. The results demonstrated that UBX-382 efficiently induced polyubiquitination and the subsequent degradation of BTK protein (Fig. 2D). Moreover, we also examined the effects of the proteasome inhibitor bortezomib, the neddylation inhibitor MLN4924, and the autophagosome-lysosome fusion inhibitor bafilomycin A1 under treatment with UBX-382 in cells. The amount of BTK remained unchanged when UBX-382 was co-treated with bortezomib or MLN4924 but not with bafilomycin A1, suggesting that BTK reduction occurs through ubiquitin-dependent proteasomal degradation (Fig. 2E). Proteomic analysis showed that only BTK and C-terminal Src kinase were reduced in as early as 4 h after treatment of UBX-382 (Fig. 2F). Overall results suggest that UBX-382 exerts highly potent and relatively selective BTK degradation through proteasomal degradation.

UBX-382 efficiently inhibits BCR downstream signaling in B-cell malignancy

To determine whether the PROTAC-induced BTK degradation affects downstream BCR signaling cellular activity, we examined anti-proliferative activity of UBX-382 against TMD-8, OCI-LY3, and U2932 cell lines. Consistent with a previous report [35], ibrutinib suppressed the growth of TMD-8 cells, showing a greater inhibitory effect than that of UBX-382. Nevertheless, UBX-382 retained superior anti-proliferative activity to that of ARQ-531, a reversible BTK inhibitor (Fig. 3A). Since both normal and malignant B cells are known to secrete CCL3 and CCL4 in response to BCR activation [36], we tried to confirm CCL3 and CCL4 secretion when BCR signaling was triggered by anti-IgM treatment in the TMD-8 cells. Treatment with 10 nM of UBX-382, ibrutinib, and acalabrutinib significantly abrogated CCL3 or CCL4 secretion, whereas treatment with ARQ-531, the BTK binder part of UBX-382 (Binder), and MT-802 initiated little or no effect, suggesting that inhibition of BCR signaling by UBX-382 decreases the production of chemokines CCL3 and CCL4 in TMD-8 cells which could disrupt tumor-microenvironment interactions in CLL patients [37] (Fig. 3B).

Next, we investigated whether UBX-382 could be applied to ibrutinib-insensitive WSU-DLCL2 (Fig. 3C) or the ibrutinib-resistant OCI-Ly3 and U2932 cell lines for anti-proliferative effect (Fig. 3D). UBX-382 showed greater inhibition than ibrutinib or ARQ-531 considering the proliferation of all three cell lines. These results indicate that UBX-382 can exert immense anti-proliferative effects on various ABC-DLBCL cell lines. We also monitored downstream BTK signaling after BCR activation in the ibrutinib-resistant U2932 cell line. Inhibition of BTK Y223 phosphorylation upon anti-IgM stimulation with UBX-382 was far more effective, compared with those of ibrutinib, acalabrutinib, and ARQ-531 in both 6 and 24 hour treated cells. (Fig. 3E). In addition, UBX-382 inhibited phosphorylation of SYK, ERK, and MEK, partially explaining its potent anti-proliferative activity in U2932 cells.

In vivo pharmacodynamics (PD) and UBX-382 efficacy

To evaluate PD profiles of UBX-382 as an orally bioavailable BTK degrader, UBX-382 was administered via PO route in the mice to monitor BTK kinetics in splenic B cells using spleens collected at 3, 8, 24, and 48 h after a single administration (Fig. 4A). BTK was rapidly degraded at 3 h with effects lasting 24 h after the administration of 30 mg/kg of UBX-382, before slowly increasing at 48 h (Fig. 4B). We further confirmed that PROTAC administration significantly reduced BTK levels in the tumors of CB17/SCID mice

of the TMD-8 xenograft model (Fig. 4C) by western blotting and immunohistochemistry (Fig. 4D and 4E). The inhibitory effects of UBX-382 on tumor growth was investigated using murine xenograft models, and the data showed that the daily oral administration of 10 or 30 mg/kg of UBX-382 for 3 weeks induced complete tumor regression within an average of 15 days (Fig. 4F). Then 30 mg/kg of UBX-382 was administered in the 3 mg/kg dose group for further 3 weeks, starting 7 days after the end of the initial experiment, resulting in total tumor regression. Although the tumors rebound in one out of nine mice in the 10 mg/kg group, this was not observed in the mice that were administered other doses until 84 days after the first administration (Fig. 4F). No weight loss or other clinical toxicity signs were observed during the experiment (Fig. 4G). These results suggest that UBX-382 shows exceptional PD efficacy and antitumor activity in mice when administered orally.

UBX-382 degrades various mutant BTK proteins *in vitro* and *in vivo*

Since resistance-associated mutations such as, E41K, T474I, several C481 and L528W BTK mutants have been found in CLL patients and in patients with Richter's transformation after ibrutinib treatment, UBX-382 was evaluated for the degradation activity against various BTK mutants for overcoming mutant resistance.

To investigate the degradation activity of UBX-382 against BTK mutants, diverse BTK mutants, such as E41K, T474I, C481S, C481R, C481T, C481Y, C481F, and L528W, were constructed (Fig. 5A). By performing transient transfection into the HEK293 cells, each BTK protein or its phosphorylated form was monitored after treatment of UBX-382, ARQ-531, and MT-802 with 0.1, 1.0, and 10 μM of each. ARQ-531 is a reversible inhibitor that suppresses BTK activation upon BCR signaling in a C481S mutational-status independent manner [32]. MT-802 is a BTK PROTAC that can degrade C481S [31]. Overall results suggest that UBX-382 effectively degrades WT and various BTK mutants, except for T474I, and strongly repressed their phosphorylation (Fig. 5B). Notably, UBX-382 appears to be far more active than ARQ-531 and MT-802 against WT and mutant BTKs.

To examine whether UBX-382 can overcome drug resistance in C481S, the anti-proliferative activities of ibrutinib and UBX-382 was compared against the parent TMD-8 cells and WT or C481S BTK-overexpressing TMD-8 cells. Overexpression of C481S BTK conferred resistance to ibrutinib treatment, which was not observed in the other TMD-8 cells. In contrast, UBX-382 significantly inhibited cell proliferation in all tested cell lines including C481S mutant (Fig. 5C).

We then used the C481S BTK-expressing TMD-8 cells in xenograft mouse models to further evaluate UBX-382 therapeutic efficacy in the ibrutinib-resistant model. To achieve this, the tumor size in each group was measured following 3 weeks of the daily administration of 3, 10, and 30 mg/kg of UBX-382, 30 mg/kg of ibrutinib, ARQ-531, and Binder via the PO route. The results indicated that UBX-382 induced remarkable tumor regression in a dose-dependent manner, whereas ibrutinib could not inhibit tumor growth, as reported (Fig. 5D and Fig. S1) [38]. This suggests that UBX-382 antitumor activity can be highly enhanced in its PROTAC form, compared with that of the Binder or ARQ-531 alone. The *in vivo* efficacy of UBX-382

was outstanding in the TMD-8 and ibrutinib-resistant xenograft models, suggesting UBX-382 as a promising therapeutic option over BTK inhibitors for the treatment of drug-resistant hematological cancers.

UBX-382 inhibits hematological cell line proliferation via CRBN dependency

Given that UBX-382 efficiently inhibits the growth of ibrutinib-sensitive and -insensitive ABC-DLBCL cells in both *in vitro* and *in vivo*, its anti-proliferative effect was examined using various types of hematological cell lines. We performed Cell Titer-Glo® 2.0 in germinal center B-cell-like diffuse large B-cell lymphoma (Su-DHL-10), follicular lymphoma (DOHH2), MCL (Mino), chronic myelogenous leukemia (K562), WSU-WM, and MOLM13 cells with UBX-382, ibrutinib, and ARQ-531 (Fig. 6A). Compared with ibrutinib and ARQ-531, UBX-382 showed superior anti-proliferative activity in all tested cell lines except WSU-SM, for which little effect was observed with all three compounds. UBX-382 greatly outperformed ibrutinib and ARQ-531 in K562, with an IC_{50} of approximately 2.2 nM. These results suggest that UBX-382 can be a promising therapeutic agent for numerous hematological disease models including DLBCL.

As UBX-382 diversely affects proliferation in various hematological cell lines, potential roles of CRBN were explored by treating U2932, TMD-8, DOHH-2, MINO, K562, and WSU-WM with UBX-382. Because the CRBN binder of UBX-382 is derived from thalidomide, we monitored the levels of Ikaros (IKZF1), Helios (IKZF2), Aiolos (IKZF3), GSPT1, and CK1-a, which are known neo-substrates of IMiD-CRBN (42-44), upon treatment with UBX-382 or thalidomide (Fig. 6B). Interestingly, BTK degradation under treatment of UBX-382 was comparable among all the cell lines, despite different growth inhibitions. No significant change was observed in the neo-substrates of U2932 and WSU-WM upon treatment with 100 nM of UBX-382 or thalidomide for 24 or 72 h, whereas degradation of CRBN neo-substrates were highly increased in TMD-8, DOHH-2, and K562 cells after treatment with UBX-382. The protein levels of CRBN neo-substrates are given graphically for each cell line (Fig. 6C). Under these conditions, thalidomide alone was not observed to produce any significant degradation in the CRBN neo-substrates for any of the tested cell lines. These results suggest that UBX-382 not only serves as a BTK degrader but also creates a cell type-dependent binding interface for targeting CRBN neo-substrates, which probably explains the diverse anti-proliferative effects among the various hematological cell lines.

Discussion

Inhibition of BCR signaling with small molecules is a well-validated strategy for the treatment of several blood cancers [39]. A recent PROTAC approach provides an alternative solution to overcome drug-induced resistance and disease relapse that result from the action of inhibitors [31]. Although several BTK-targeting PROTACs have been described recently [40], none of them showed *in vivo* efficacy against in both WT and C481S mutant. We developed a potent and orally available BTK PROTAC, UBX-382, with remarkable degradation activity and excellent PD profiles for efficient cancer-targeting activity in WT and C481S mutant. The effect of UBX-382 on tumor inhibition could be further mediated through CRBN responses depending on hematological cell types.

One of the most well-known advantages of the PROTAC modality is its ability to overcome the drug resistance that results from mutation. Ibrutinib has been used successfully in several hematological and chronic graft-versus-host diseases [41]. As BTK inhibition by ibrutinib relies on its irreversible binding to the C481 site in the ATP binding pocket, BTK mutations at C481 will inevitably affect ibrutinib-treated patients [12–14]. Moreover, E41K and T474I BTK mutants were also found in CLL patients after ibrutinib treatment, and L528W is another BTK mutant found in patients with Richter's transformation [42]. In particular, E41K BTK, a constitutively active and gain-of-function mutant, can promote trans-autophosphorylation of BTK kinase domain and lead to over-proliferation of malignant cells [43, 44]. Here, we explored the inhibitory activities of UBX-382, ARQ-531, and MT-802 against five C481 mutants (C481S, C481R, C481Y, C481T, and C481F) and three other mutants (E41K, T474I, and L528W) of BTK. ARQ-531 is an ATP-competitive and reversible inhibitor that does not interact with C481, theoretically suggesting that C481 mutants do not interfere with its inhibitory activity. As previously reported [32], BTK phosphorylation was substantially attenuated in ARQ-531-treated C481S and E41K BTK mutants (Fig. 5B). However, the other six BTK mutants were only slightly affected by ARQ-531 when in phosphorylated form. By contrast, MT-802 and UBX-382 PROTACs were competent in phosphorylation degradation and suppression in the WT and most of BTK mutants, highlighting an advantage of PROTACs over active-site-directed inhibitors. Notably, UBX-382 outperformed MT-802 in WT and all sensitive BTK mutants, while L528W was sensitive only to the treatment of UBX-382. The T474I mutant was resistant to all three BTK-targeting compounds used [45]. The *in vitro* potency of UBX-382 in degradation of BTK mutant was also reflected in the *in vivo* tumor growth inhibition of a murine xenograft model using C481S-expressing TMD-8 cells (Fig. 5D). Therefore, UBX-382 could provide an alternative solution for the patients of hematological cancers with diverse BTK mutants acquired from treatment of the first- or second-line BTK inhibitors.

Another merit of the PROTAC modality is maximization of target inhibition by event-driven proteolysis, compared with conventional inhibitors [27, 46]. Although the molecular weight of UBX-382 is approximately two times higher than that of the Binder, UBX-382 showed more prominent antitumor activity than the Binder and other BTK inhibitors upon the administration of the same dose (30 mg/kg) in the *in vivo* mouse models (Fig. 5D). A similar phenomenon was reported for ARV-771 PROTAC and JQ1 binders [47]. Therefore, our data showed that efficacies from PROTAC-induced degradation could exceed activities from the Binder, which may be strongly advantageous considering dose reduction in clinical conditions.

In particular, while complete degradation of BTK was observed both *in vitro* and *in vivo* as a result of UBX-382 treatment, degradation patterns of CRBN neo-substrates were variable in a cell type-dependent manner in all cell lines used, to some extent complying with a recent report on tissue-specific differences of the BTK-degrader effect [48]. We speculate that this cell type-dependent CRBN effect may occur under different environments of ubiquitination system. Diverse expression level of the POI and CRBN may affect the ratio of productive PROTAC-containing ternary complexes to neo-substrate-targeting IMiD-CRBN complexes. This stoichiometric alteration might also be determined by neddylation of cullin complex, deubiquitinating activities, or other unknown host factors. Hematological cell lines may respond

differently to signaling pathways such as NF-κB, BCR-ABL, Janus kinase–signal transducer and activator of transcription, PI3K/Akt/mTOR, and/or MAPK [49, 50], which might differentially reprogram cellular networks such as the ubiquitin-proteasome machinery.

Conclusions

Overall, UBX-382 is potent in inducing BTK degradation, which can be applied in various hematological *in vitro* disease models. UBX-382 also exhibited outstanding degradation potency against various mutant BTKs, expanding its application feasibility to patients with recurrent cancers who have received prior treatment of BTK inhibitors. Furthermore, oral administration of UBX-382 exhibited excellent *in vivo* efficacy in murine xenograft models using BTK WT- and mutant-expressing ABC-DLBCL cellsSince UBX-382 degrades BTK as well as diverse CRBN neo-substrates depending on cell lines, it could be applicable for the tailored treatment of B-cell malignancies. The compelling results of UBX-382 as a highly potent and efficient degrader suggest that UBX-382 could be a promising preclinical candidate for various hematological malignancies.

List Of Abbreviations

Bruton's tyrosine kinase (BTK); B-cell receptor (BCR); chronic lymphocytic leukemia/small lymphocytic lymphoma (CLL/SLL); Waldenström's macroglobulinemia (WM); relapsed/refractory mantle cell lymphoma (R/R MCL); relapsed/refractory marginal zone lymphoma (R/R MZL); proteolysis-targeting chimeras (PROTACs); ubiquitin-proteasome system (UPS); protein of interest (POI); von Hippel-Lindau (VHL); cereblon (CRBN); immunomodulatory drugs (IMiDs); Ikaros (IKZF1); Helios (IKZF2); Aiolos (IKZF3); casein kinase 1-a (CK1-a); G1 to S phase transition protein 1 (GSPT1); glutathione-S-transferase (GST); N-2-hydroxyethylpiperazine-N'-2-ethanesulfonic acid (HEPES); fluorescence resonance energy transfer (FRET); half-maximal inhibitory concentration (IC_{50}); room temperature (RT); time-resolved FRET (TR-FRET); homogeneous TR-FRET (HTRF); sodium dodecyl sulfate–polyacrylamide gel electrophoresis (SDS-PAGE); tris(hydroxymethyl)aminomethane (Tris); Tris-buffered saline and Tween 20 (TBST); immunoglobulin (Ig); phosphate-buffered saline (PBS); tandem ubiquitin-binding elements (TUBE); C-C motif chemokine ligand (CCL); enzyme-linked immunosorbent assay (ELISA); pharmacodynamics (PD).

Declarations

Ethics approval and consent to participate

Consent for publication

Availability of data and materials

All data are available in the main text or supplementary materials.

Competing interests

Patent 10-2021-0083326 is held on UBX-382. A patent application on this work has been filed by Ubix Therapeutics, Inc. on behalf of the authors.

Funding

- This research was supported by a grant of the Korea Health Technology R&D Project through the Korea Health Industry Development Institute (KHIDI), funded by the Ministry of Health & Welfare, Republic of Korea (grant number : HI20C1021).

- This work was in part supported by Korea Research Institute of Chemical Technology (KK1931-10 and IIT20-11).

- This work was supported by the National Research Foundation of Korea (NRF) grant and the DGIST program of the Ministry of Science and ICT of Korea (2022R1A4A2000703 & 22-CoE-BT-04) to B.-H.L.

Authors' contributions

HHK measured CRBN or BTK-binding activity. YL, SY, HK, BS, JP, and NJ performed experiments and designed experiments, analyzed data, assembled, and wrote the manuscript together with SL and SY. BL and JR revised and wrote this paper. CHP established stable cell lines. VBP and PK designed and synthesized the PROTACs. SL supervised these experiments.

Acknowledgments

We thank all employees of Ubix Therapeutics, Inc.

Authors' information (optional)

References

1. Cancer Facts & Figs. 2021, American Cancer Society, 2021.
2. Morton LM, Wang SS, Devesa SS, Hartge P, Weisenburger DD, Linet MS. Lymphoma incidence patterns by WHO subtype in the United States, 1992–2001. Blood. 2006;107:265–76.
3. Burger JA, Wiestner A. Targeting B cell receptor signalling in cancer: preclinical and clinical advances. Nat Rev Cancer. 2018;18:148–67.
4. Shinners NP, Carlesso G, Castro I, Hoek KL, Corn RA, Woodland RT, et al. Bruton's tyrosine kinase mediates NF-kappa B activation and B cell survival by B cell-activating factor receptor of the TNF-R family. J Immunol. 2007;179:3872–80.
5. Dolmetsch RE, Lewis RS, Goodnow CC, Healy JI. Differential activation of transcription factors induced by Ca2 + response amplitude and duration. Nature. 1997;386:855–8.
6. Aw A, Brown JR. Current status of Bruton's tyrosine kinase inhibitor development and use in B-cell malignancies. Drugs Aging. 2017;34:509–27.

7. Wen T, Wang J, Shi Y, Qian H, Liu P. Inhibitors targeting Bruton's tyrosine kinase in cancers: drug development advances. Leukemia. 2021;35:312–32.
8. Wu J, Zhang M, Liu D. Acalabrutinib (ACP-196): a selective second-generation BTK inhibitor. J Hematol Oncol. 2016;9:21.
9. Tam CS, LeBlond V, Novotny W, Owen RG, Tedeschi A, Atwal S, et al. A head-to-head Phase III study comparing zanubrutinib versus ibrutinib in patients with Waldenström macroglobulinemia. Future Oncol. 2018;14:2229–37.
10. Sedlarikova L, Petrackova A, Papajik T, Turcsanyi P, Kriegova E. Resistance-associated mutations in chronic lymphocytic leukemia patients treated with novel agents. Front Oncol. 2020;10:894.
11. Lewis KL, Cheah CY. Non-covalent BTK inhibitors-The new BTKids on the block for B-cell malignancies. J Pers Med. 2021;11:764.
12. Woyach JA, Furman RR, Liu TM, Ozer HG, Zapatka M, Ruppert AS, et al. Resistance mechanisms for the Bruton's tyrosine kinase inhibitor ibrutinib. N Engl J Med. 2014;370:2286–94.
13. Woyach JA, Ruppert AS, Guinn D, Lehman A, Blachly JS, Lozanski A, et al. BTKC481S-mediated resistance to ibrutinib in chronic lymphocytic leukemia. J Clin Oncol. 2017;35:1437–43.
14. Xu L, Tsakmaklis N, Yang G, Chen JG, Liu X, Demos M, et al. Acquired mutations associated with ibrutinib resistance in Waldenström macroglobulinemia. Blood. 2017;129:2519–25.
15. Collins I, Wang H, Caldwell JJ, Chopra R. Chemical approaches to targeted protein degradation through modulation of the ubiquitin-proteasome pathway. Biochem J. 2017;474:1127–47.
16. Sakamoto KM, Kim KB, Kumagai A, Mercurio F, Crews CM, Deshaies RJ. Protacs: chimeric molecules that target proteins to the Skp1-Cullin-F box complex for ubiquitination and degradation. Proc Natl Acad Sci U S A. 2001;98:8554–9.
17. Gadd MS, Testa A, Lucas X, Chan KH, Chen W, Lamont DJ, et al. Structural basis of PROTAC cooperative recognition for selective protein degradation. Nat Chem Biol. 2017;13:514–21.
18. Schneekloth AR, Pucheault M, Tae HS, Crews CM. Targeted intracellular protein degradation induced by a small molecule: En route to chemical proteomics. Bioorg Med Chem Lett. 2008;18:5904–8.
19. Qi SM, Dong J, Xu ZY, Cheng XD, Zhang WD, Qin JJ. PROTAC: An effective targeted protein degradation strategy for cancer therapy. Front Pharmacol. 2021;12:692574.
20. Frost J, Galdeano C, Soares P, Gadd MS, Grzes KM, Ellis L, et al. Potent and selective chemical probe of hypoxic signalling downstream of HIF-α hydroxylation via VHL inhibition. Nat Commun. 2016;7:13312.
21. Fischer ES, Böhm K, Lydeard JR, Yang H, Stadler MB, Cavadini S, et al. Structure of the DDB1-CRBN E3 ubiquitin ligase in complex with thalidomide. Nature. 2014;512:49–53.
22. Saenz DT, Fiskus W, Qian Y, Manshouri T, Rajapakshe K, Raina K, et al. Novel BET protein proteolysis-targeting chimera exerts superior lethal activity than bromodomain inhibitor (BETi) against post-myeloproliferative neoplasm secondary (s) AML cells. Leukemia. 2017;31:1951–61.

23. Itoh Y, Kitaguchi R, Ishikawa M, Naito M, Hashimoto Y. Design, synthesis and biological evaluation of nuclear receptor-degradation inducers. Bioorg Med Chem. 2011;19:6768–78.
24. Demizu Y, Okuhira K, Motoi H, Ohno A, Shoda T, Fukuhara K, et al. Design and synthesis of estrogen receptor degradation inducer based on a protein knockdown strategy. Bioorg Med Chem Lett. 2012;22:1793–6.
25. Lai AC, Toure M, Hellerschmied D, Salami J, Jaime-Figueroa S, Ko E, et al. Modular PROTAC design for the degradation of oncogenic BCR-ABL. Angew Chem Int Ed Engl. 2016;55:807–10.
26. Gao S, Wang S, Song Y. Novel immunomodulatory drugs and neo-substrates. Biomark Res. 2020;8:2.
27. Lai AC, Crews CM. Induced protein degradation: an emerging drug discovery paradigm. Nat Rev Drug Discov. 2017;16:101–14.
28. Pettersson M, Crews CM. PROteolysis TArgeting Chimeras (PROTACs) - Past, present and future. Drug Discov Today Technol. 2019;31:15–27.
29. Sun X, Gao H, Yang Y, He M, Wu Y, Song Y, et al. PROTACs: great opportunities for academia and industry. Signal Transduct Target Ther. 2019;4:64.
30. Leiser D, Pochon B, Blank-Liss W, Francica P, Glück AA, Aebersold DM, et al. Targeting of the MET receptor tyrosine kinase by small molecule inhibitors leads to MET accumulation by impairing the receptor downregulation. FEBS Lett. 2014;588:653–8.
31. Buhimschi AD, Armstrong HA, Toure M, Jaime-Figueroa S, Chen TL, Lehman AM, et al. Targeting the C481S ibrutinib-resistance mutation in Bruton's tyrosine kinase using PROTAC-mediated degradation. Biochemistry. 2018;57:3564–75.
32. Reiff SD, Mantel R, Smith LL, Greene JT, Muhowski EM, Fabian CA, et al. The BTK inhibitor ARQ 531 targets ibrutinib-resistant CLL and richter transformation. Cancer Discov. 2018;8:1300–15.
33. Hendriks RW, Yuvaraj S, Kil LP. Targeting Bruton's tyrosine kinase in B cell malignancies. Nat Rev Cancer. 2014;14:219–32.
34. Burslem GM, Smith BE, Lai AC, Jaime-Figueroa S, McQuaid DC, Bondeson DP, et al. The advantages of targeted protein degradation over inhibition: An RTK case study. Cell Chem Biol. 2018;25:67–77.e3.
35. Paul J, Soujon M, Wengner AM, Zitzmann-Kolbe S, Sturz A, Haike K, et al. Simultaneous inhibition of PI3Kδ and PI3Kα induces ABC-DLBCL regression by blocking BCR-dependent and -independent activation of NF-κB and AKT. Cancer Cell. 2017;31:64–78.
36. Takahashi K, Sivina M, Hoellenriegel J, Oki Y, Hagemeister FB, Fayad L, et al. CCL3 and CCL4 are biomarkers for B cell receptor pathway activation and prognostic serum markers in diffuse large B cell lymphoma. Br J Haematol. 2015;171:726–35.
37. Niemann CU, Herman SE, Maric I, Gomez-Rodriguez J, Biancotto A, Chang BY, et al. Disruption of in vivo chronic lymphocytic leukemia tumor-microenvironment interactions by ibrutinib–findings from an investigator-initiated phase II study. Clin Cancer Res. 2016;22:1572–82.

38. Sun Y, Ding N, Song Y, Yang Z, Liu W, Zhu J, et al. Degradation of Bruton's tyrosine kinase mutants by PROTACs for potential treatment of ibrutinib-resistant non-Hodgkin lymphomas. Leukemia. 2019;33:2105–10.
39. Burger JA. Inhibiting B-cell receptor signaling pathways in chronic lymphocytic leukemia. Curr Hematol Malig Rep. 2012;7:26–33.
40. George B, Chowdhury SM, Hart A, Sircar A, Singh SK, Nath UK, et al. Ibrutinib resistance mechanisms and treatment strategies for B-cell lymphomas. Cancers (Basel). 2020;12:E1328.
41. de Claro RA, McGinn KM, Verdun N, Lee SL, Chiu HJ, Saber H, et al. FDA approval: Ibrutinib for patients with previously treated mantle cell lymphoma and previously treated chronic lymphocytic leukemia. Clin Cancer Res. 2015;21:3586–90.
42. Gángó A, Alpár D, Galik B, Marosvári D, Kiss R, Fésüs V, et al. Dissection of subclonal evolution by temporal mutation profiling in chronic lymphocytic leukemia patients treated with ibrutinib. Int J Cancer. 2020;146:85–93.
43. Li T, Tsukada S, Satterthwaite A, Havlik MH, Park H, Takatsu K, et al. Activation of Bruton's tyrosine kinase (BTK) by a point mutation in its pleckstrin homology (PH) domain. Immunity. 1995;2:451–60.
44. Wang Q, Pechersky Y, Sagawa S, Pan AC, Shaw DE. Structural mechanism for Bruton's tyrosine kinase activation at the cell membrane. Proc Natl Acad Sci U S A. 2019;116:9390–9.
45. Sharma S, Galanina N, Guo A, Lee J, Kadri S, Van Slambrouck C, et al. Identification of a structurally novel BTK mutation that drives ibrutinib resistance in CLL. Oncotarget. 2016;7:68833–41.
46. Li X, Song Y. Proteolysis-targeting chimera (PROTAC) for targeted protein degradation and cancer therapy. J Hematol Oncol. 2020;13:50.
47. Raina K, Lu J, Qian Y, Altieri M, Gordon D, Rossi AM, et al. PROTAC-induced BET protein degradation as a therapy for castration-resistant prostate cancer. Proc Natl Acad Sci U S A. 2016;113:7124–9.
48. Nguyen TM, Deb A, Kokkonda P, Sreekanth V, Tiwari PK, Shoba V, et al. Proteolysis targeting chimeras with reduced off-targets. bioRxiv. 2021.
49. Wang H, Hu H, Zhang Q, Yang Y, Li Y, Hu Y, et al. Dynamic transcriptomes of human myeloid leukemia cells. Genomics. 2013;102:250–6.
50. Trojani A, Di Camillo B, Bossi LE, Leuzzi L, Greco A, Tedeschi A, et al. Identification of a candidate gene set signature for the risk of progression in IgM MGUS to Smoldering/Symptomatic Waldenström macroglobulinemia (WM) by a comparative transcriptome analysis of B cells and plasma cells. Cancers (Basel). 2021;13:1837.

Figures

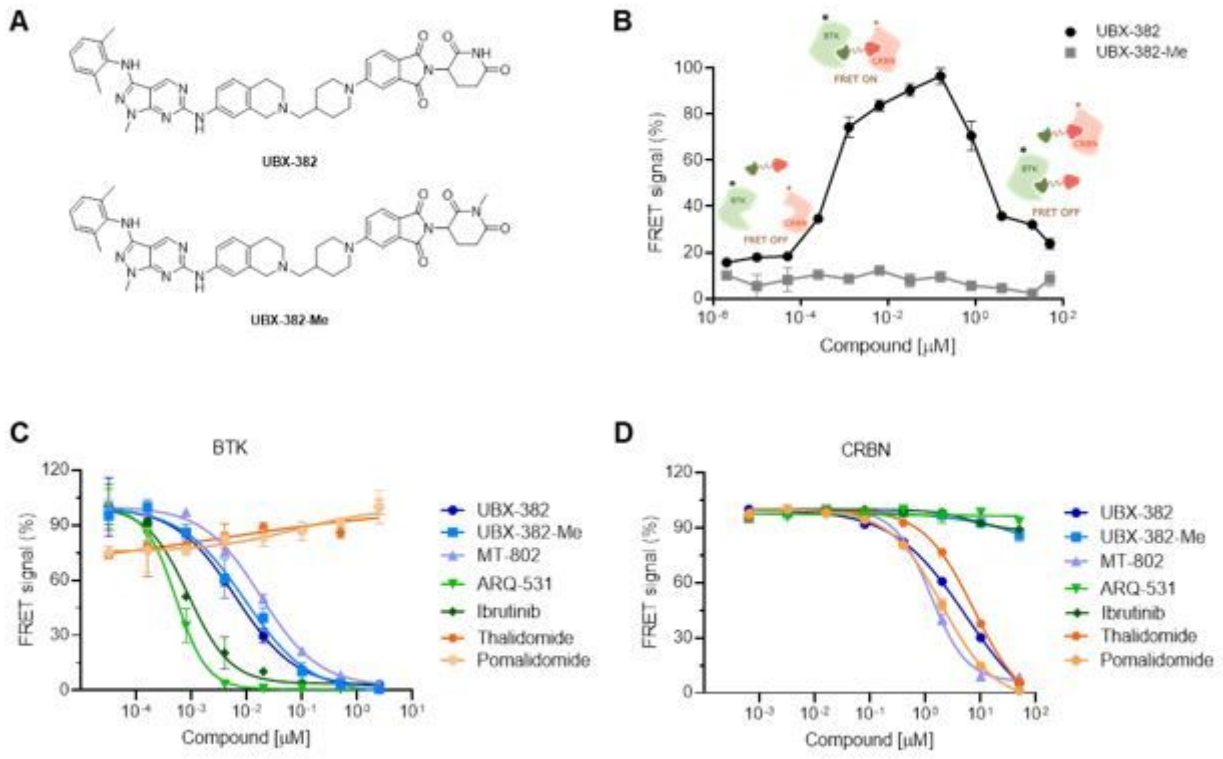

Compounds	IC_{50} (nM)
UBX-382	6.312
UBX-382-Me	9.351
MT-802	18.11
ARQ-531	0.521
Ibrutinib	0.882
Thalidomide	ND
Pomalidomide	ND

Compounds	IC_{50} (μM)
UBX-382	5.511
UBX-382-Me	ND
MT-802	1.258
ARQ-531	ND
Ibrutinib	ND
Thalidomide	7.612
Pomalidomide	1.991

Figure 1

In vitro target binding assay

(A) Chemical structures of UBX-382 and UBX-382-Me. (B) TR-FRET based *in vitro* [BTK:PROTAC:CRBN] ternary complex formation assay for UBX-382 and UBX-382-Me. Relative FRET signals represent the normalized mean of FRET signals from two replicates. histidine-tagged (12 nM) and GST-tagged (20 nM) were incubated with 12 different concentrations within the range 0.002048 nM ~ 50000 nM for 30 min and collected at 620 nm (donor) and 665 nm (acceptor). (C) BTK-target binding assay for UBX-382 (navy circle), UBX-382-Me (blue square), MT-802 (light blue pyramid), ARQ-531 (green inverted pyramid), ibrutinib (dark green diamond), thalidomide (orange hexagon), and pomalidomide (beige circle). IC_{50} values of 6.31, 9.35, 18.11, 0.52, 0.88, not determined (ND), and ND were obtained for UBX-382, UBX-382-Me, MT-802, ARQ-531, ibrutinib, thalidomide, and pomalidomide, respectively. (D) CRBN-target binding assay for UBX-382 (navy circle), UBX-382-Me (blue square), MT-802 (light blue pyramid), ARQ-531 (green

inverted pyramid), ibrutinib (dark green diamond), thalidomide (orange hexagon), and pomalidomide (beige circle). IC_{50} values of 5.51, ND, 1.26, ND, ND, 7.61, and 1.99 were obtained for UBX-382, UBX-382-Me, MT-802, ARQ-531, ibrutinib, thalidomide, and pomalidomide, respectively. Data are represented as the mean values ± standard deviation.

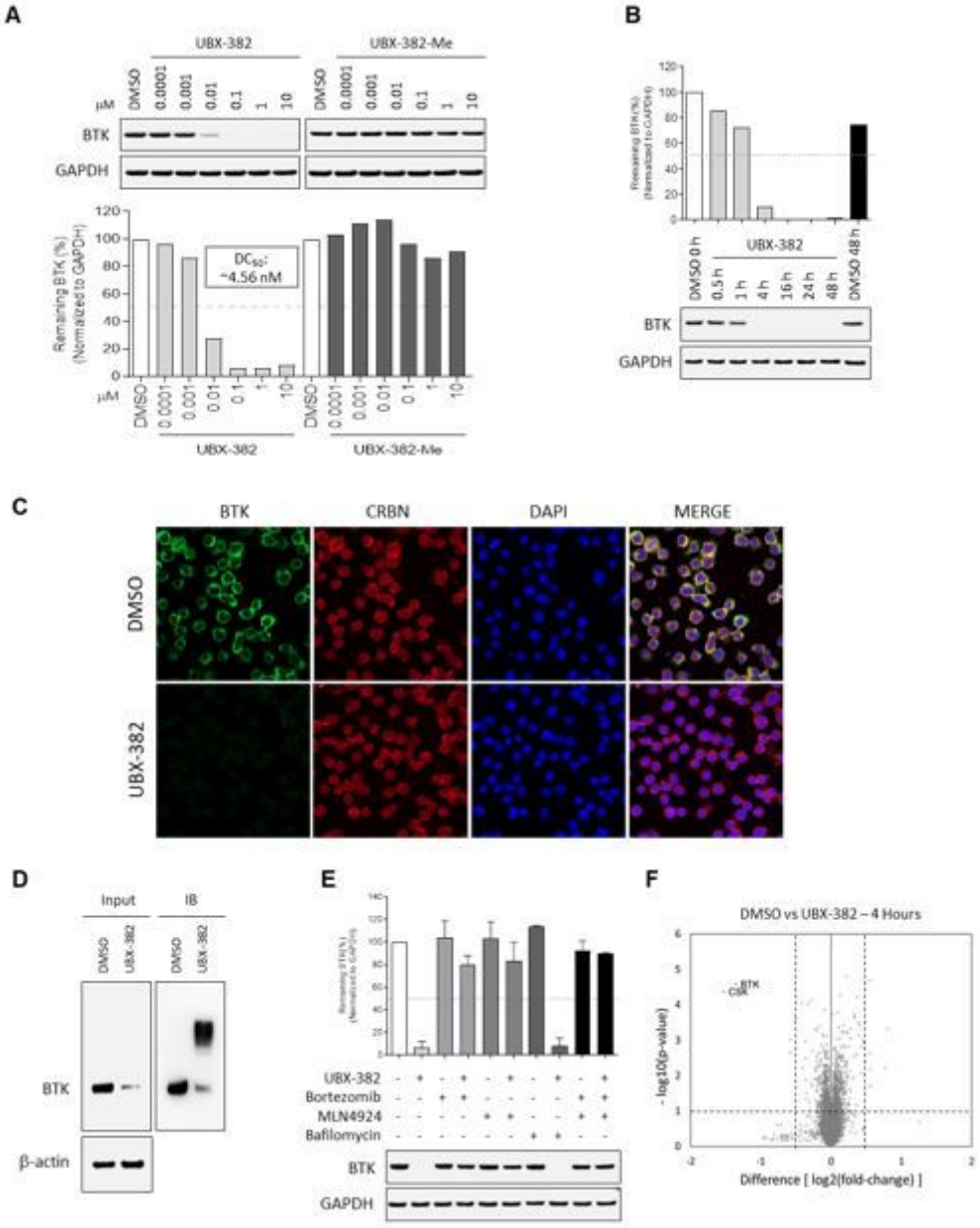

Figure 2

UBX-382 potently degrades BTK via proteasome action in B-cell malignant cell lines (A) BTK degradation in response to increasing UBX-382 and UBX-382-Me doses in TMD-8 cells over 24 h. BTK levels were measured by immunoblotting using specific antibodies and values for the remaining BTK were normalized using glyceraldehyde-3-phosphate dehydrogenase (GAPDH) intensity as a loading control. (B) Immunoblotting analysis of time-dependent degradation of BTK by treatment with UBX-382 in TMD-8

cells. The cells were treated with 100 nM UBX-382 for 0.5, 1, 4, 16, 24, and 48 h and harvested for the analysis of BTK levels using BTK antibodies. The remaining BTK values were normalized using GAPDH intensity as a loading control. (C) The degradation effect of BTK by UBX-382 as determined by immunofluorescence analysis in the TMD-8 cells. Variations in BTK levels and CRBN as a result of treatment with UBX-382 for 24 h were observed by immunofluorescence using specific antibodies as indicated in *Materials and Methods*. The TMD-8 cells were visualized using a confocal microscope (400×) Green, BTK; red, CRBN; and blue, nucleus. Scale bars, 20 μm. (D) BTK polyubiquitination was induced by treatment with 100 nM UBX-382 for 2 h in Ramos cells. The polyubiquitin chains on BTK were observed using TUBE1 pull-down experiments as described in *Materials and Methods*. GAPDH was used to confirm an equal amount of protein loading. (E) BTK degradation is mediated by the UPS in TMD-8 cells. The TMD-8 cells were pretreated with 0.1 μM bortezomib, MLN4924, or bafilomycin for 1 h and then treated with 0.1 μM UBX-382 for 4 h. Immunoblotting was performed to verify BTK levels using specific antibodies. The immunoblotting results represented two independent experiments ($n = 2$). Data are expressed as the mean ± standard error of the mean. (F) Quantitative proteomics analysis was performed to evaluate proteome changes in TMD-8 cells. The cells were treated with 100 nM UBX-382 or dimethyl sulfoxide (DMSO) for 4 h. Lysates were treated with the TMT-6 plex kit, which was followed by liquid chromatography-tandem mass spectrometry-based proteomics analysis. Volcano plot indicates protein ranking per the abundance ratio ($\log_2$ fold change) for DMSO and UBX-382 and the statistical *p*-value. The non-axial vertical line represents a fold change of ±1.5 and the non-axial horizontal line indicates a *p*-value of 0.05 significance threshold. This experiment was performed in triplicates. A total of 7418 proteins were identified in this experiment.

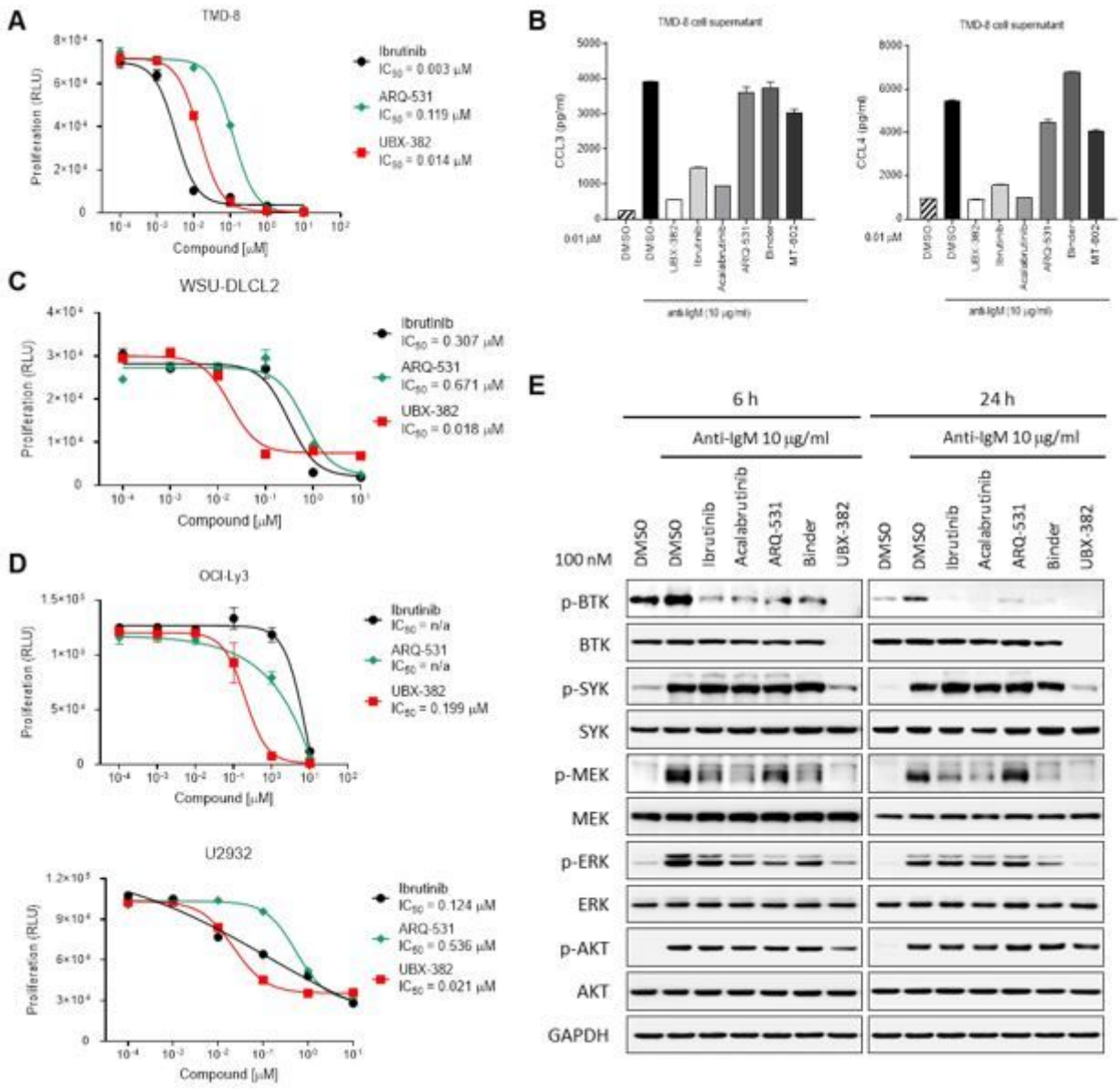

Figure 3

Inhibitory effects of UBX-382 on BCR-mediated downstream signaling

(A) Evaluation of inhibitory effects on cell proliferation by ibrutinib (black circle), ARQ-531 (green diamond), and UBX-382 (red square) in TMD-8 cells. The cells were seeded and treated with increasing doses of ibrutinib, ARQ-531, and UBX-382 for 3 days. Cell proliferation was measured by the Cell Titer-Glo assay in duplicates. Data are expressed as the mean ± standard error of the mean. (B) Secreted CCL3 and CCL4 levels in the TMD-8 cells. Secretion of CCL3 (left) and CCL4 (right) by the TMD-8 cells following anti-IgM stimulation for 8 h and 10 nM UBX-382, ibrutinib, acalabrutinib, ARQ-531, Binder, or MT-802 for 24 h. Each graph indicates the mean concentration of CCL3 and CCL4 produced by the TMD-8 cells cultured in a medium with dimethyl sulfoxide, UBX-382, ibrutinib, acalabrutinib, ARQ 531, Binder, or MT-802 in the presence of 10 μg/mL anti-IgM. The experiments were performed in duplicates. Data represent

the mean ± standard error of the mean. (C, D) Comparison of anti-proliferative effect following treatment with ibrutinib (black circle), ARQ-531 (green diamond), and UBX-382 (red square) in WSU-DLCL2, OCI-Ly3, or U2932 cells. The cells were seeded and treated with increasing concentrations of ibrutinib, ARQ-531, and UBX-382 for 5 days. The assay was performed in duplicates. Data are expressed as the mean ± standard error of the mean. (E) Suppression of BCR-mediated signaling axis by UBX-382. U2932 cells were treated with 100 nM ibrutinib, acalabrutinib, ARQ-531, Binder, and UBX-382 for 6 and 24 h and stimulated with 10 μg/mL anti-IgM for 15 min. Phosphorylation and total protein levels of BTK, SYK, MEK, and ERK were visualized via immunoblotting using indicated specific antibodies. Glyceraldehyde-3-phosphate dehydrogenase was used as a loading control.

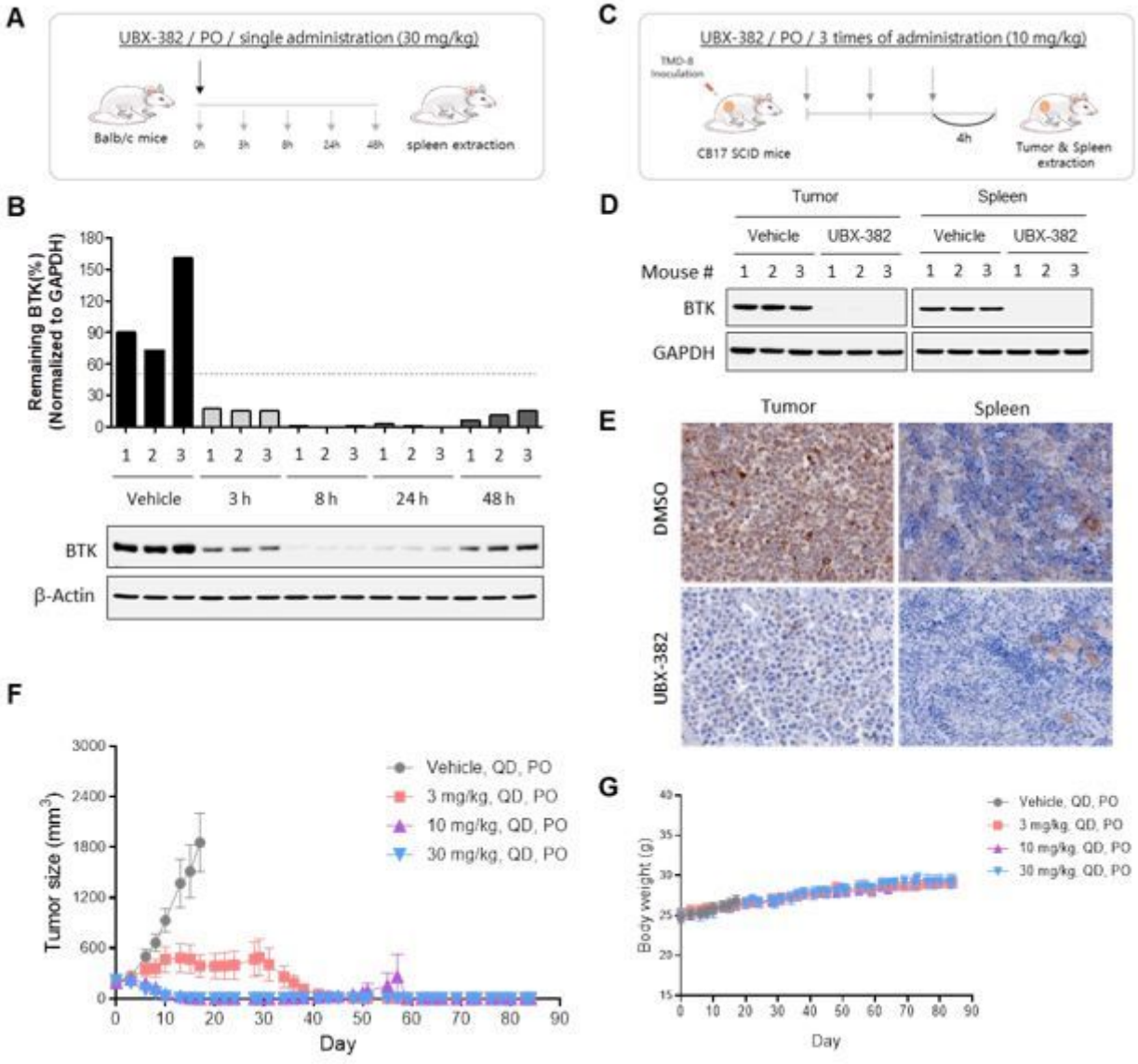

Figure 4

Evaluation of PD effect of UBX-382 *in vivo*

(A) Schematic overview of *in vivo* PD experimental design. (B) BTK levels at each dosing time (3, 8, 24, and 48 h) were observed in spleen tissues extracted from mice (*n = 3* per group). (C) Experimental scheme of *in vivo* PD experimental design in the xenograft model. (D) Western blot analysis of BTK levels in tumor and spleen samples of vehicle or UBX-382 treated group, *n = 3* per group. (E) Immunohistochemical study of BTK levels in TMD-8 tumor and spleen tissues treated with dimethyl sulfoxide or UBX-382. Paraffin sections of the tissues were visualized by 3,3-diaminobenzidine staining (*n = 3* per group). (F) Graph showing tumor size following UBX-382 administration in the TMD-8 xenograft mouse models, with nine mice in each group. Xenograft mice were subjected to oral UBX-382 (3, 10, and 30 mg/kg) for 3 weeks. UBX-382 was re-administered to the 3 mg/kg group at a concentration of 30 mg/kg for 3 weeks 7 days after the discontinuation of the original dosing. (G) Bodyweight of CB17 SCID mice treatment groups with TMD-8 xenografts after dosing with vehicle or UBX-382 (*n = 9* per group). Data describing tumor growth and body weight are presented as the mean ± standard error of the mean.

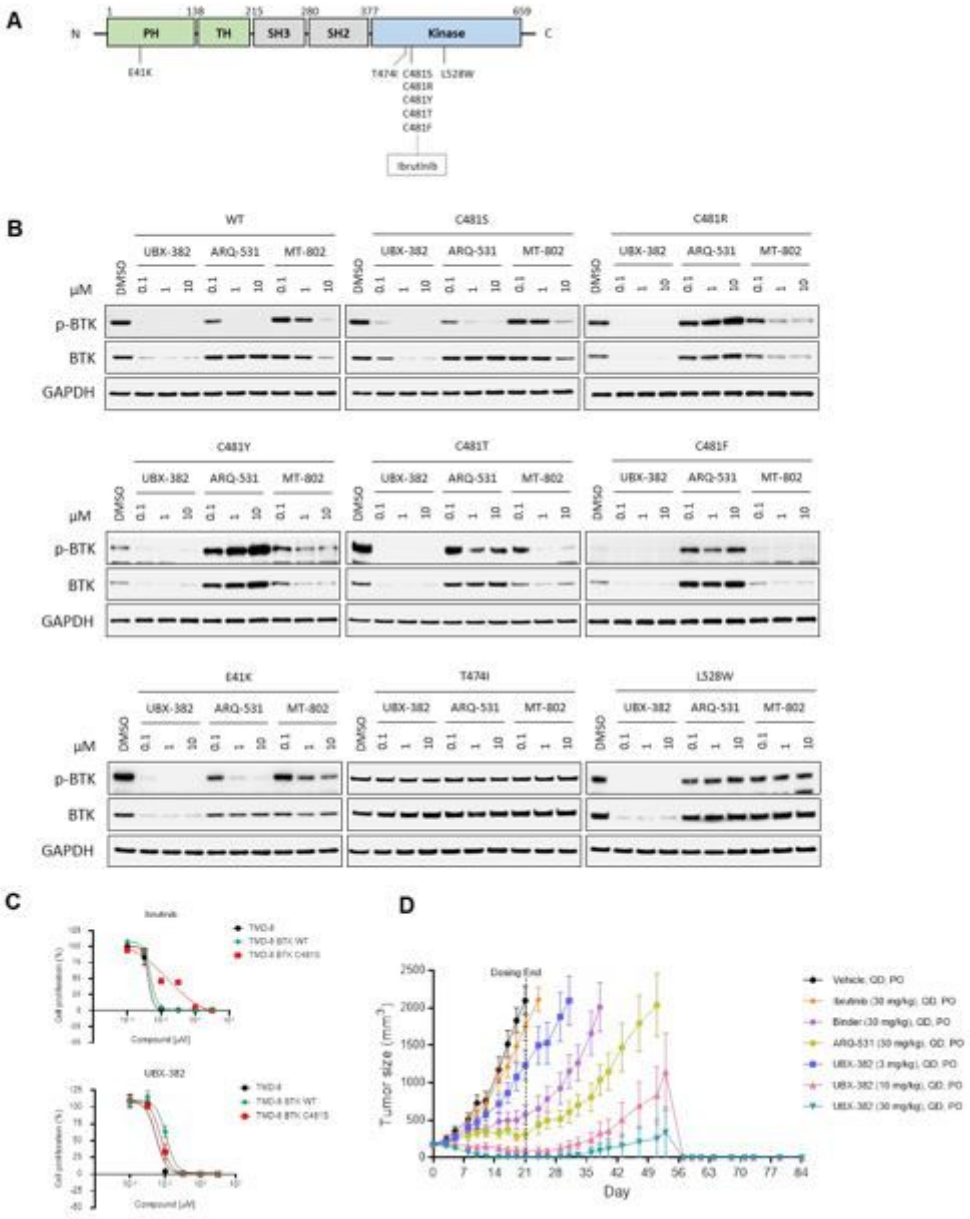

Figure 5

Potent degradation and inhibition of mutated BTK *in vitro* and *in vivo* with UBX-382 treatment

(A) Schematic domain structure of BTK with known mutant sites (B) Transient expressing WT or various mutant BTK in HEK293 cells were treated with UBX-382, ARQ-531, or MT-802 for 24 h in a concentration-dependent manner (0.1, 1, and 10 μM). BTK levels and Y223 phosphorylation were visualized by immunoblotting. Glyceraldehyde-3-phosphate dehydrogenase was used as an internal loading control. Data were obtained from two independent experiments (n = 2). (C) Parental TMD-8 cells, WT-, or C481S BTK overexpressed TMD-8 cells were treated with the indicated concentration of ibrutinib or UBX-382 for 5 days to measure the inhibitory effect on proliferation. These experiments were performed in duplicates by Cell Titer-Glo® 2.0 Assay. Data are presented as the mean ± standard error of the mean (SEM). (D) UBX-382 showed antitumor effects in TMD-8 BTK C481S *in vivo* models and induced tumor remission.

TMD-8 BTK C481S cells were inoculated subcutaneously into the right flank of male CB17 SCID mice. When tumors had reached over 180–200 mm^3, the mice were divided into seven groups and subjected to oral treatment with a control vehicle (*n* = 7), ibrutinib (30 mg/kg, *n* = 7), Binder (30 mg/kg, *n* = 7), ARQ-531 (30 mg/kg, *n* = 7), and UBX-382 (3, 10, 30 mg/kg, *n* = 7), respectively, each day for 21 days. Tumor volume (mean ± SEM) was observed for 84 days.

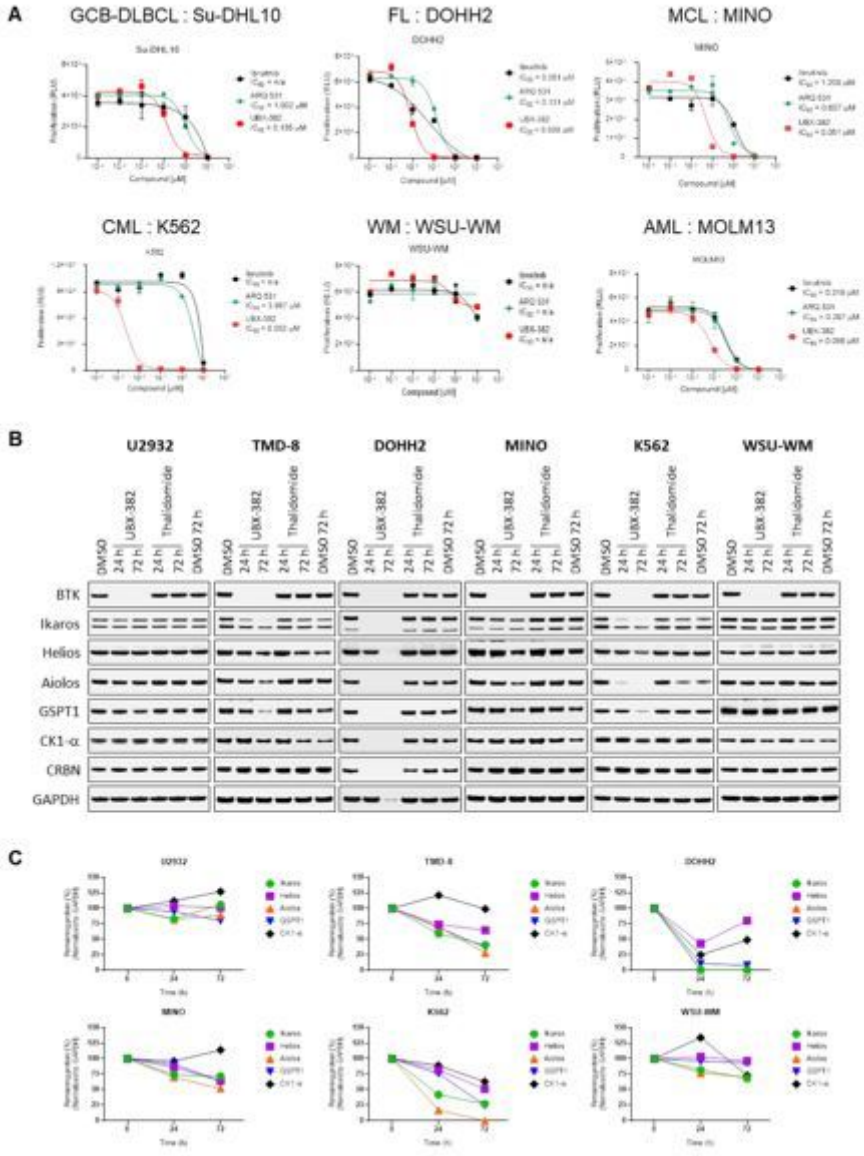

Figure 6

Validation of the anti-proliferative activity of UBX-382 in diverse cell lines derived from hematological malignancies

(A) Inhibitory effects of ibrutinib (black circle), ARQ-531 (green diamond), and UBX-382 (red square) on cell proliferation in the examined cell lines at the indicated increasing doses were monitored for 5 days by

performing Cell Titer-Glo® 2.0 Assay. Germinal center B-cell-like diffuse large B-cell lymphoma cell line: Su-DHL10; multiple myeloma cell line: U266; follicular lymphoma cell line: DOHH2; MCL cell line: MINO; chronic myeloid leukemia cell line: K562; acute myeloid leukemia cell line: MOLM13. Experiments were performed in duplicates. All data are expressed as the mean ± SEM. (B) Immunoblotting analysis of BTK degradation and CRBN neo-substrates after treatment with UBX-382 and thalidomide. Hematological cell lines (U2932, TMD-8, DOHH2, MINO, K562, and WSU-WM) were treated with 100 nM thalidomide and UBX-382 for 24 h and 72 h. Immunoblotting was performed to verify the levels of BTK, Ikaros, Helios, Aiolos, GSPT1, and CK1-α using specific antibodies. (C) CRBN neo-substrate protein levels were measured by immunoblotting and values of the remaining substrates, Ikaros, Aiolos, GSPT1, and CK1-α, were normalized using glyceraldehyde-3-phosphate dehydrogenase intensity value as a loading control.

Supplementary Files

This is a list of supplementary files associated with this preprint. Click to download.

- SupplementaryDataJournalofHematologyOncology.docx